

Morphological modifications of C_{60} crystal rods under hydrothermal conditions

Ming-Run Du(杜明润), Shi-Xin Liu(刘士鑫), Jia-Jun Dong(董家君), Ze-Peng Li(李泽朋), Ming-Chao Wang (王明超), Tong Wei(魏通), Qing-Jun Zhou(周青军), Xiong Yang(杨雄), and Peng-fei Shen(申鹏飞)

Citation: Chin. Phys. B, 2020, 29 (**12**): 128102. DOI: 10.1088/1674-1056/abc0
Journal homepage: http://cpb.iphy.ac.cn; http://iopscience.iop.org/cpb

What follows is a list of articles you may be interested in

Crystallization and characteristics of {100}-oriented diamond with CH_4N_2S additive under high pressure and high temperature

Yong Li(李勇), Debing Tan(谭德斌), Qiang Wang(王强), Zhengguo Xiao(肖政国), Changhai Tian(田昌海), Lin Chen(陈琳)

Chin. Phys. B, 2020, 29 (**9**): 098103. DOI: 10.1088/1674-1056/ab99b9

Facile and fast growth of high mobility nanoribbons of $ZrTe_5$

Jingyue Wang(王璟岳), Jingjing Niu(牛晶晶), Xinqi Li(李新祺), Xiumei Ma(马秀梅), Yuan Yao(姚湲), Xiaosong Wu(吴孝松)

Chin. Phys. B, 2020, 29 (**6**): 068102. DOI: 10.1088/1674-1056/ab889a

Modulation of magnetic and electrical properties of bilayer graphene quantum dots using rotational stacking faults

Hong-Ping Yang(杨宏平), Wen-Juan Yuan(原文娟), Jun Luo(罗俊), Jing Zhu(朱静)

Chin. Phys. B, 2019, 28 (**7**): 078106. DOI: 10.1088/1674-1056/28/7/078106

Path integral Monte Carlo study of $(H_2)_n@C_{70}$ (n=1,2,3)

Hao Yan, Zhang Hong, Cheng Xin-Lu

Chin. Phys. B, 2015, 24 (**8**): 088103. DOI: 10.1088/1674-1056/24/8/088103

Optoelectronic characteristics of CuO nanorods

Xie De-Hua, Wang Fei-Fei, Lü Hao, Du Min-Yong, Xu Wen-Jie

Chin. Phys. B, 2013, 22 (**5**): 058103. DOI: 10.1088/1674-1056/22/5/058103

Morphological modifications of C_{60} crystal rods under hydrothermal conditions*

Ming-Run Du(杜明润)[1], Shi-Xin Liu(刘士鑫)[1], Jia-Jun Dong(董家君)[2], Ze-Peng Li(李泽朋)[1,†], Ming-Chao Wang (王明超)[1], Tong Wei(魏通)[1], Qing-Jun Zhou(周青军)[1], Xiong Yang(杨雄)[1], and Peng-fei Shen(申鹏飞)[3]

[1] *College of Science, Civil Aviation University of China, Tianjin* 300300, *China*
[2] *State Key Laboratory of Superhard Materials, College of Physics, Jilin University, Changchun* 130012, *China*
[3] *Academy for Advanced Interdisciplinary Studies, Southern University of Science and Technology, Shenzhen* 519055, *China*

(Received 8 June 2020; revised manuscript received 28 August 2020; accepted manuscript online 14 October 2020)

We observed morphological modification of rod-shaped C_{60} solvate crystals using a facile hydrothermal method. The initial C_{60} rods were changed from smooth rods to rough rods, porous rods or pieces under different hydrothermal conditions. During the hydrothermal treatment, the initial samples underwent a decomposition-recrystallization process, which can be tuned by the content of alcohol in the hydrothermal solution, thereby leading to modification of the morphological properties of the initial C_{60} rods. In addition, the rough and porous C_{60} rods prepared in our work exhibit excellent photoluminescence intensities that are approximately 7 and 3 times higher than those of pure C_{60} powders, respectively. Our results suggest that the hydrothermal method is a potential route for fabricating fullerene materials with controllable morphologies and novel functions.

Keywords: fullerene crystals, morphological modification, porous materials, hydrothermal method

PACS: 81.05.ub, 81.10.–h, 81.05.Rm, 61.48.–c **DOI:** 10.1088/1674-1056/abc0d8

1. Introduction

Fullerenes exhibit fascinating physical and chemical properties owing to their unique closed-cage molecular structures, and provide promising applications in fabricating functional devices such as organic solar cells, light-emitting diodes, field effect transistors, and sensors, for which syntheses of well-defined fullerene molecular assemblies are required to achieve high performance.[1–12] On the other hand, their engineering unique properties are strongly dependent on the ability to control the structure, size and morphology of fullerene materials, which remain a crucial issue in fullerene nanoscience and nanotechnology as well as applications.[13] Therefore, investigation on preparation of crystalline fullerenes with controllable morphology is of great interest from both a fundamental and a practical point of view.

To date, several methods such as the solution-phase crystallization method, vapor deposition method and template method have been introduced to fabricate high-quality fullerene nanocrystals with various morphologies, including one-dimensional (1D) nanorods, whiskers or nanotubes, 2D sheets or disks, and 3D cubes.[14–29] Among these methods, the solution-phase crystallization method attracts the most interest because the morphologies of the products can be easily tailored by adjusting various parameters.[23–29] For example, Kim *et al.* reported a simple reprecipitation method for controlling the morphology of C_{70} crystals to be either cubic or tubular not by replacing specific solvents but by simply controlling the volume ratio of C_{70}-mesitylene to isopropyl alcohol.[23] Sathish *et al.* found that the size of hexagonal C_{60} nanosheets crystallized at the CCl_4/alcohol interface could be tailored merely by changing the alcohol to isopropyl alcohol or methanol.[24] Tan *et al.* observed a shape transformation of solvated C_{60} microcrystals from an as-grown bundle shape to a disk shape by utilizing a mild thermal treatment in the solvent medium.[25] Wei *et al.* synthesized single-crystal ultrathin microribbons of $2C_{60}{\cdot}3CS_2$ by mixing the poor solvent isopropyl alcohol with a C_{60}/CS_2 stock solution, while the as-formed microribbons transformed to prismatic rods after being kept in mother liquid under ambient conditions over weeks.[28] Masuhara *et al.* experimentally demonstrated the cyclic transformations in shape (rod shape→hexagonal disc shape→rod shape) of C_{60} solvated crystals in dispersion by changing the dispersion solvent medium and keeping the dispersion under supersonic irradiation.[29] However, the solution-phase crystallization method generally requires storage of fullerene crystals in toxic organic solutions. Moreover, fullerene materials derived from the solution phase usually entrap solvent molecules in their lattices (i.e., crystallization from the solu-

*Project supported by the National Natural Science Foundation of China (Grant Nos. 11804384, 51802343, and 51772326), the Fundamental Research Funds for the Central Universities, China (Grant No. 3122018L006), the Scientific Research Project of Tianjin Education Commission (Grant No. 2019ZD19), the National Natural Science Foundation of China and the Civil Aviation Administration of China (Grant No. U1933109), and Open Project of State Key Laboratory of Superhard Materials (Jilin University) (Grant No. 201803).

†Corresponding author. E-mail: li_zepeng@163.com

© 2020 Chinese Physical Society and IOP Publishing Ltd

tion phase produces fullerene solvated structures).[23,25,28–31] These facts limit the practical applications of fullerene crystals prepared by such a method in functional devices. Thus, exploring an efficient and environmentally friendly method for preparing fullerene crystals with controllable morphology and high purity (constituted with pure fullerene) is still needed.

Recently, mesoporous C_{70} cubes with highly crystalline frameworks were prepared by a mild heat treatment of C_{70} cubes, fabricated by the liquid-liquid interfacial precipitation (LLIP) method, in mother liquor at 75 °C.[26] Such porous materials exhibit excellent photoluminescence (PL) properties and higher specific capacitance than those of pristine C_{70} due to the larger electrochemically active surface areas. Furthermore, highly ordered mesoporous C_{60} rods with well-ordered porous structures and a high degree of crystallinity were obtained through the nanohard templating method, which offers high supercapacitive performance and high selectivity for H_2O_2 production as well as methanol tolerance for oxygen reduction reactions.[32] These interesting results suggest that the introduction of well-defined porous architectures with controllable pore sizes into fullerene nanostructures not only increases their surface areas but also provides additional functionalities, suggesting their utility in several applications including supercapacitors, hydrogen storage, photocatalysts and sensing. The synthesis of novel porous fullerene crystals will open a new avenue in research on porous carbon nanomaterials and enable the discovery and exploration of novel crystalline porous materials useful in various applications.

It is well known that the hydrothermal method is an efficient route to synthesize nanocrystals and materials with porous structures in aqueous solution by providing high-temperature and high-pressure conditions.[33] However, such a method is rarely used for the preparation of fullerene nanocrystals. In this work, we study the behaviors of 1D rod-shaped C_{60} solvated crystals in aqueous solutions with different alcohol amounts under hydrothermal conditions. Our aim is to investigate the possible morphology, structure and property modifications of C_{60} rods during hydrothermal treatment and to attempt to synthesize pure C_{60} nanocrystals with controllable morphology, especially porous structures, by a hydrothermal approach. Such knowledge should contribute to the exploration of new methods for fabricating nanostructured fullerene materials with controllable morphologies and novel functions.

2. Experiments

2.1. Materials synthesis

Fullerene powders (C_{60}, purity 99.9%) were purchased from Nanjing XFNANO Materials TECH Co., Ltd. The initial C_{60} rods were fabricated by introducing isopropyl alcohol (IPA, isopropanol) into a saturated solution of C_{60} in m-xylene. In brief, 30 mL IPA was injected into 10 mL saturated C_{60}/m-xylene solution (∼3 mg/mL) followed by 1 min ultrasonication. After 24 h, brown deposits were precipitated on the bottom of the solution bottle. The as-synthesized samples were collected by filtration and dried under ambient conditions. In a typical process for preparing hydrothermally derived C_{60} samples, 6 mg initial C_{60} rods, as precursors, were added into 30 mL deionized water followed by 1 min ultrasonication to form a C_{60} rod aqueous dispersion. After injecting a certain volume (0, 1, 2 mL) of alcohol (≥ 99.7%, Beijing Chemical Works) into the dispersion, the mixture was transferred into a Teflon-lined stainless steel autoclave (50 ml capacity), filling the autoclave up to 60% of the total volume. The autoclave was maintained at 120 °C for 18 h under autogenerated pressure. The resulting products were collected by filtration, washed thoroughly several times with deionized water, and dried under ambient conditions prior to characterization. More experimental details about the material synthesis are shown in Fig. S1 in the Supplementary Material.

2.2. Characterization

The morphologies and structures of the hydrothermally derived C_{60} samples and initial C_{60} rods were characterized with scanning electron microscopy (SEM, FEI Magellan 400), transmission electron microscopy (TEM, JEM-2200FS transmission electron microscopy with an acceleration voltage of 200 kV) and x-ray diffraction (XRD, RigakuD/max-RA, Cu $K\alpha 1$ radiation with $\lambda = 1.5406$ Å (Rigaku, Tokyo, Japan)). Raman and PL spectra of the samples were measured with a Raman spectrometer (Renishaw in Via (Renishaw, London, UK)) excited by a 514 nm laser. IR measurements were carried out using a Bruker Vertex 80 V Fourier transform infrared spectroscopy (FTIR) spectrometer.

3. Results and discussion

Figure 1 shows the SEM images of initial C_{60} rods and hydrothermally derived C_{60} samples prepared at 120 °C for 18 h from C_{60} rod aqueous dispersions (30 mL deionized water, 6 mg C_{60} rods) with different injected volumes of alcohol. It is found that the initial C_{60} rods have an average diameter and length of ∼ 0.221 μm and 1.55 μm, respectively (Fig. 1(a) and Fig. S2). In comparison to the initial C_{60} rods, the samples prepared from the dispersion without injecting alcohol are still rod-shaped, but with a slightly smaller average diameter of ∼0.210 μm and rough surfaces (Fig. 1(b) and Fig. S3). After the hydrothermal treatment, the C_{60} products obtained from the dispersion injected with 1 ml alcohol retain the rod-shaped appearance of the precursors, while many pores (the average pore size is ∼27 nm, Fig. S4(a)) are found on their surfaces. This result indicates the transformation of initial

C_{60} rods into porous materials during the hydrothermal process (Fig. 1(c)). The average diameter of the achieved porous C_{60} rods is ~0.208 μm (Fig. S4(b)). To the best of our knowledge, this is the first example of porous fullerene materials fabricated by a simple hydrothermal approach. It should be noted that the diameters of the hydrothermally derived rough and porous C_{60} rods are similar to those of initial C_{60} rods, indicating that the formation mechanisms of these two hydrothermally derived samples are straightforward. As shown in Fig. 1(d), the hydrothermally treated initial C_{60} rods from the dispersion injected with 2 ml alcohol crack into pieces that lack well-defined morphologies. These SEM results of the hydrothermally derived C_{60} samples suggest that the hydrothermal method is a potential route for tailoring the morphologies of fullerene crystals.

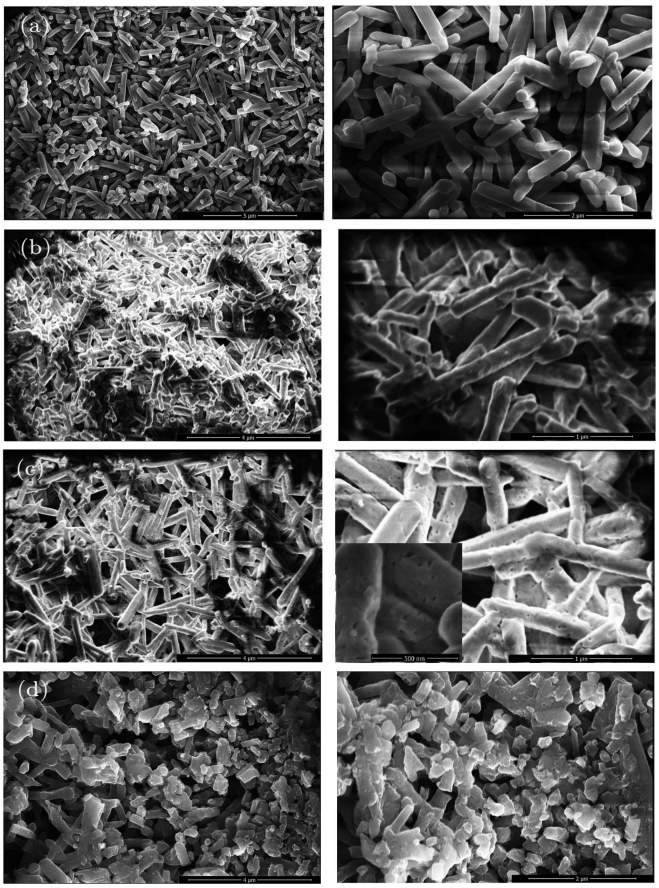


Fig. 1. SEM images of initial C_{60} rods (a), rough C_{60} rods (b), porous C_{60} rods (c) and C_{60} crystal pieces (d). Inset: the enlarged SEM image of the porous C_{60} rods.

To detect the possible structural transformations of the initial C_{60} rods under hydrothermal conditions, we performed Raman and IR spectroscopies, x-ray diffraction and high-resolution TEM (HRTEM) measurements on the hydrothermally derived C_{60} samples. Raman and IR spectroscopies are powerful methods for characterizing carbon materials.[34,35] The Raman and IR spectra of the hydrothermally derived C_{60} samples are shown in Figs. 2(a) and 2(b). For comparison, the vibrational spectra of the initial C_{60} rods are also presented at the bottom of the figures. From the figure, we can find that the Raman spectra of the four samples are almost identical, which mainly consist of 10 Raman modes (8 Hg modes and 2 Ag modes) from individual C_{60} molecules.[14,21,22,36,37] The IR spectrum of initial C_{60} rods show clear spectroscopic features from both m-xylene molecules (absorption peak at around 773 cm^{-1}) and C_{60} molecules (three F_{1u} modes at around 575 cm^{-1}, 1182 cm^{-1} and 1428 cm^{-1}), indicating that solvents remain in the rods. In contrast, the solvent peak is absent in the IR spectra of hydrothermally derived samples, which only consist of the spectroscopic features from pure C_{60}.[14,22] These observations suggests that the intermolecular interactions in the samples are weak van der Waals interactions, thus excluding the formation of C_{60} polymers or derivatives during the hydrothermal process.[21,22,34,38] Furthermore, the absence of solvent peak in the IR spectra of the hydrothermally derived samples suggests the desolvation of initial C_{60} rods upon the hydrothermal treatments.[14,39] Note that the solvent molecules in fullerene solvates interact through weak supramolecular forces so that they can be released upon heat treatment.[22,25,26,39] The crystal forms of the hydrothermally derived C_{60} samples and the initial C_{60} rods are established by powder XRD (Fig. 2(c)). A mixed phase of fcc ($a = 14.13(7)$ Å) and hcp is observed for the initial C_{60} rods, confirming their solvated structures.[14,22,26,39] It was reported that C_{60} forms solid solvates with the solvent m-xylene by solvent evaporation or the LLIP method, exhibiting an hcp structure with lattice parameters $a = 2.37(6)$ Å and $c = 1.00(8)$ Å.[14,22,39,40] On the other hand, all the hydrothermally derived C_{60} samples transform into an fcc structure similar to that of pure C_{60} crystals (fcc, $a = 14.15(6)$ Å).[39] This result implies that the crystal structure of the initial C_{60} rods is destabilized and that most of the entrapped m-xylene molecules in the rods escape from the lattices during the hydrothermal process. HRTEM images and the corresponding fast Fourier transform (FFT) images indicate the crystalline nature of the hydrothermally derived C_{60} samples, which are consistent with the XRD results (Fig. S5)

We further studied the PL properties of the hydrothermally derived C_{60} samples. The recorded PL spectra of the hydrothermally derived C_{60} samples, initial C_{60} rods and pure C_{60} powders, for comparison, are shown in Fig. 3. From the figure, we can find that all the samples exhibit a similar red emission, with the strongest emission band located at approximately 1.66 eV. The main component of such PL emission can be assigned to the S_1–S_0 transition of the C_{60} molecule.[22,41] Of the studied hydrothermally derived C_{60} samples, the rough C_{60} rods exhibit the most intense PL, similar to that of the initial C_{60} rods, which is approximately 7 times greater than that

of the pure C_{60} powders. The PL intensity of the porous C_{60} rods is reduced, while it is still at least approximately 3 times higher than that of the pure C_{60} powders. This finding suggests that porous C_{60} rods are also highly PL active, which may be utilized in potential applications such as sensors, photoreceptors, and lighting devices.[26,41] The obvious PL enhancements observed in the rough and porous C_{60} rods in comparison to the pure C_{60} powders can be attributed to their highly crystalline structures.[41] For the C_{60} crystal pieces, their PL intensity is the lowest and is comparable to that of pure C_{60} powders. This observation may imply that the C_{60} crystal pieces have the lowest crystallinity.[26,41]

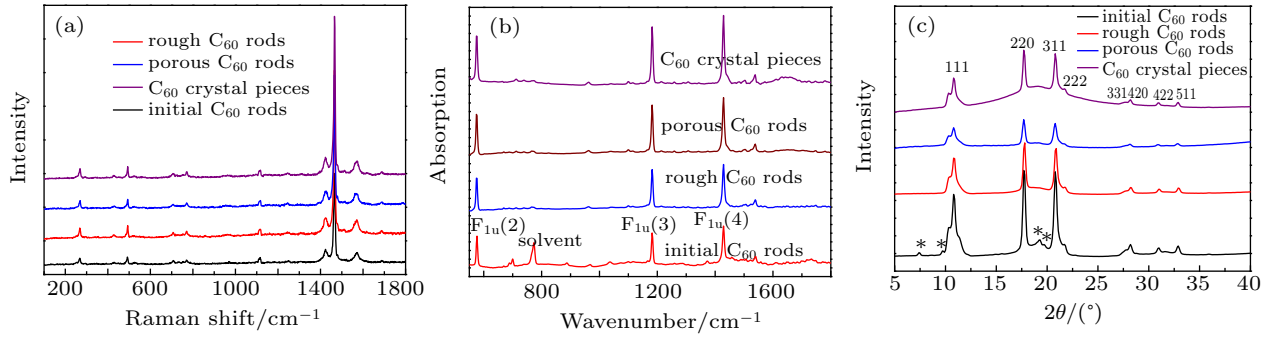


Fig. 2. The Raman spectra (a), IR spectra (b) and XRD patterns (c) of hydrothermally derived C_{60} samples in comparison to those of initial C_{60} rods. The diffraction peaks assigned to the hcp structure of C_{60} solvates are marked with asterisks in the figure.

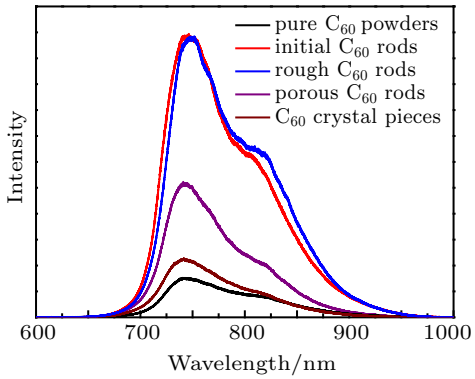


Fig. 3. The PL spectra of the hydrothermally derived C_{60} samples in comparison to those of initial C_{60} rods and pure C_{60} powders.

Let us now discuss the mechanisms for the morphological modifications of the initial C_{60} rods during the hydrothermal processes. As indicated in our Raman, IR and XRD results, the initial C_{60} rods transform into an fcc structure, and the entrapped m-xylene solvent molecules can be released from the initial solvated lattice upon hydrothermal treatment at 120 °C, which leads to structure destabilization and void spaces in the solids.[25,26] It is reported that thermal treatment could induce phase and morphology transformations of solvated C_{60} microcrystals by three steps in solvent medium (ethanol or 2-propanol): exchange of incorporated solvent, decomposition of old crystals, and recrystallization of dislocated C_{60} molecules into new crystals.[25] Furthermore, C_{60} nanowires were reported to be destabilized and transformed to granular C_{60} crystals over time in solution containing water.[42] These facts suggest that the hydrothermal treatments in aqueous or aqueous-alcohol solution could reduce the crystal stability of the initial C_{60} rods and induce partial decomposition or recrystallization of these samples, thereby leading to morphological modifications of the initial C_{60} rods. Under hydrothermal treatment in an aqueous solution without alcohol, only a tiny quantity of C_{60} molecules can be released from the surfaces of initial C_{60} rods due to the structural destabilization induced by water. This leads to partial decomposition of the rod surfaces, and thus resulting in the transformation of initial samples into rough C_{60} rods. As was reported, C_{60} molecules are almost insoluble in water but slightly soluble in alcohol.[30] The injection of 1 mL alcohol increases the solubility of C_{60} in the C_{60} rod aqueous dispersion. On the other hand, under hydrothermal treatment in an aqueous solution containing 1 mL alcohol solvated C_{60} molecules on the surface of initial C_{60} rods can exchange the incorporated solvent ligands by entrapping (releasing) ethanol (m-xylene) molecules.[25] This exchange together with the increased solubility of C_{60} in the dispersion destabilize the crystal structure of the initial C_{60} rods and induce dissolution of more C_{60} molecules from the surface during the hydrothermal process. In such cases, the initial sample begins to decompose, and many defects form on the samples and may serve as active sites for recrystallization of dislocated C_{60} molecules, thereby modifying the morphology of the initial C_{60} rods and leading to the formation of a porous structure.[25,26] When the injected volume of alcohol increases to 2 mL, the hydrothermally treated initial C_{60} rods decompose into C_{60} crystal pieces with low crystallinity due to the higher solubility of C_{60} molecules in the dispersion and the formation of more structural defects on the treated samples.

4. Conclusion

In conclusion, the morphological modification of rod-shaped C_{60} solvated crystals has been realized by hydrothermal treatment at 120 °C for 18 h. It is found that the content of injected alcohol in the hydrothermal solution plays an important role in the morphological modification by tuning the decomposition-recrystallization process of the initial C_{60} rods

under hydrothermal conditions. During the hydrothermal process, the structural destabilization induced by water, the increasing solubility of C_{60} molecules in the hydrothermal solution and the formation of structural defects on the initial C_{60} rods due to the injection of alcohol lead to decomposition and recrystallization of the treated initial samples, thereby modifying the morphology of the initial C_{60} rods. Strikingly, rod-shaped C_{60} crystals with porous and fcc structures have been successfully prepared by hydrothermal methods. Such porous C_{60} rods exhibit excellent PL intensity ($\sim$3 times higher intensity than that of pure C_{60} powders) due to their high degree of crystallinity, which could have potential applications in sensors, photoreceptors, and lighting devices. These results may facilitate the development of a new route with great potential for fabricating fullerene materials with controllable morphologies and novel functions via simple hydrothermal approaches.

References

[1] Briseno A L, Mannsfeld S C B, Ling M M, Liu S, Tseng R J, Reese C, Roberts M E, Yang Y, Wudl F and Bao Z 2006 *Nature* **444** 913

[2] Dresselhaus M S, Dresselhaus G and Eklund P C 1996 *Science of Fullerenes and Carbon Nanotubes* (San Diego: Academic Press) pp. 437–438

[3] Kim J Y, Lee K, Coates N E, Moses D, Nguyen T Q, Dante M and Heeger A J 2007 *Science* **317** 222

[4] Dennler G, Scharber M C and Brabec C J 2009 *Adv. Mater.* **21** 1323

[5] Lai Y Y, Cheng Y J and Hsu C S 2014 *Energy Environ. Sci.* **7** 1866

[6] Deng L L, Xie S Y and Gao F 2018 *Adv. Electron. Mater.* **4** 1700435

[7] Sun X N, Velez S, Atxabal A, Bedoya-Pinto A, Parui S, Zhu X, Llopis R, Casanova F and Hueso L E 2017 *Science* **357** 677

[8] Anthony J E, Facchetti A, Heeney M, Marder S R and Zhan X W 2010 *Adv. Mater.* **22** 3876

[9] Li H Y, Tee B C K, Cha J J, Cui Y, Chung J W, Lee S Y and Bao Z N 2012 *J. Am. Chem. Soc.* **134** 2760

[10] Yuan Y Y, Han S, Grozea D and Lu Z H 2006 *Appl. Phys. Lett.* **88** 093503

[11] Jariwala D, Sangwan V K, Lauhon L J, Marks T J and Hersam M C 2013 *Chem. Soc. Rev.* **42** 2824

[12] Shi X L, Liu S R, Sun Y, Liang J J and Chen Y S 2018 *Adv. Funct. Mater.* **28** 1800850

[13] Yao M G, Du M R and Liu B B 2013 *Chin. Phys. B* **22** 098109

[14] Wang L, Liu B B, Liu D, Yao M G, Hou Y Y, Yu S D, Cui T, Li D L, Zou G T, Iwasiewicz A and Sundqvist B 2006 *Adv. Mater.* **18** 1883

[15] Vimalanathan K, Shrestha R G, Zhang Z, Zou J, Nakayama T and Raston C L 2017 *Angew. Chem. Int. Ed.* **56** 8398

[16] Briseno A L, Mannsfeld S C B M, Ling M, Liu S, R. TsengJ, Reese C, Roberts M E, Yang Y, Wudl F and Bao Z 2006 *Nature* **444** 913

[17] Sathish M, Miyazawa K, Hill J P and Ariga K 2009 *J. Am. Chem. Soc.* **131** 6372

[18] Kim J, Park C, Song I, Lee M, Kim H and Choi H C 2016 *Sci. Rep.* **6** 32205

[19] Nair V S, Mukhopadhyay R D, Saeki A, Seki S and Ajayaghosh A 2016 *Sci. Adv.* **2** e1600142

[20] Liu H B, Li Y L, Jiang L, Luo H Y, Xiao S Q, Fang H J, Li H M, Zhu D B, Yu D P and Xiang B 2002 *J. Am. Chem. Soc.* **124** 13370

[21] Yao M G, Andersson B M, Stenamrk P, Sundqvist B, Liu B B and Wagberg T 2009 *Carbon* **47** 1181

[22] Wang L, Liu B B, Yu S D, Yao M G, Liu D D, Hou Y Y, Cui T and Zou G T 2006 *Chem. Mater.* **18** 4190

[23] Kim J, Park C and Choi H C 2015 *Chem. Matter* **27** 2408

[24] Sathish M and Miyazawa K 2007 *J. Am. Chem. Soc.* **129** 13816

[25] Tan Z Q, Masuhar A, Kasai H, Nakanishi H and Oikawa H 2013 *Carbon* **64** 370

[26] Bairi P, Tsuruoka T, Acharya S, Ji Q M, Hill J P, Ariga K, Yamauchi Y and Shrestha L K 2018 *Mater. Horiz.* **5** 285

[27] Park C, Song H J and Choi H C 2009 *Chem. Commun.* **2009** 4803

[28] Wei L, Yao J N and Fu H B 2013 *ACS Nano* **7** 7573

[29] Masuhara A, Tan Z Q, Ikeshima M, Sato T, Kasai H, Oikawa H and Nakanishi H 2012 *CrystEngComm* **14** 7787

[30] Marcus Y, Smith A L, Korobov M V, Mirakyan A L, Avramenko N V and Stukalin E B 2001 *J. Phys. Chem. B* **105** 2499

[31] Sivaraman N, Dhamodaran R, Kaliappan I, Srinivasan T G, Vasudeva Rao P R P and Mathews C K C 1994 *Fullerene Sci. Technol.* **2** 233

[32] Benzigar M, Joseph S, Ilbeygi H, Park D H, Sarkar S, Chandra G, Umapathy S, Srinivasan S, Talapaneni S N and Vinu A 2018 *Angew. Chem. Int. Ed.* **57** 569

[33] Huang H, Zhu W J, Tao X Y, Xia Y, Yu Z Y, Fang J W, Gan Y P and Zhang W K 2012 *ACS Appl. Mater. Interfaces* **4** 5974

[34] Du M R, Yao M G, Dong J J, Ge P, Dong Q, Kováts É, Pekker S, Chen S L, Liu R, Liu B, Cui T, Sundqvist B and Liu B B 2018 *Adv. Mater.* **30** 1706916

[35] Dong J J, Yao Z, Yao M G, Li R, Hu K, Zhu L Y, Wang Y, Sun H H, Sundqvist B, Yang K and Liu B B 2020 *Phys. Rev. Lett.* **124** 065701

[36] Bethune D S, Meijer G, Tang W C and Rosen H J 1991 *Chem. Phys. Lett.* **179** 181

[37] Wang K A, Wang Y, Zhou P, Holden J M, Ren S L, Hager G T, Ni H F, Eklund P C, Dresselhaus G and Dresselhaus M S 1992 *Phys. Rev. B* **45** 1995(R)

[38] Suchanek W L, Libera J A, Gogotsi Y and Yoshimura M 2001 *J. Solid State Chem.* **160** 184

[39] Liu D D, Wang L, Cui W, Yao M G, Li Q J, Li Z P, Zou B, Cui T, Liu B B and Sundqvist B 2011 *Diam. Relat. Mater.* **20** 178

[40] Minato J I, Miyazawa K 2005 *Carbon* **43** 2837

[41] Penterman S J, Singh A, Zipfel W R and Liddell Watson C M 2014 *Adv. Opt. Mater.* **2** 1024

[42] Miyazawa K C and Hotta K J 2011 *Nanopart. Res.* **13** 5739